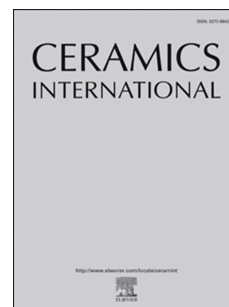


Journal Pre-proof

Significant enhancement on creep resistance of the near stoichiometric SiC fibers by ultrafast Joule heating

Litipu Aihaiti, Shuxing Li, Dilare Halmurat, Jiajing Zhou, Siwei Li, Rong-Jun Xie



PII: S0272-8842(24)06078-4

DOI: <https://doi.org/10.1016/j.ceramint.2024.12.403>

Reference: CERI 44687

To appear in: *Ceramics International*

Received Date: 17 October 2024

Revised Date: 6 December 2024

Accepted Date: 24 December 2024

Please cite this article as: L. Aihaiti, S. Li, D. Halmurat, J. Zhou, S. Li, R.-J. Xie, Significant enhancement on creep resistance of the near stoichiometric SiC fibers by ultrafast Joule heating, *Ceramics International*, <https://doi.org/10.1016/j.ceramint.2024.12.403>.

This is a PDF file of an article that has undergone enhancements after acceptance, such as the addition of a cover page and metadata, and formatting for readability, but it is not yet the definitive version of record. This version will undergo additional copyediting, typesetting and review before it is published in its final form, but we are providing this version to give early visibility of the article. Please note that, during the production process, errors may be discovered which could affect the content, and all legal disclaimers that apply to the journal pertain.

© 2024 Published by Elsevier Ltd.

Significant enhancement on creep resistance of the near stoichiometric SiC fibers by ultrafast Joule heating

Litipu Aihaiti ^a, Shuxing Li ^a, Dilare Halmurat ^a, Jiajing Zhou ^a,

Siwei Li ^{a, c*}, Rong-Jun Xie ^{a, b**}

^a College of Materials, Xiamen University, Xiamen, Fujian 361005, China

^b State Key Laboratory of Physical Chemistry of Solid Surface, College of Materials, Xiamen University, Xiamen 361005, China

^c Key Laboratory of High Performance Ceramic Fibers (Xiamen University), Ministry of Education, Xiamen 361005, China.

* Corresponding author at: Key Laboratory of High Performance Ceramic Fibers (Xiamen University), Ministry of Education, Xiamen 361005, China. E-mail addresses: swli@xmu.edu.cn (S. Li).

** Corresponding author at: College of Materials, Xiamen University, Xiamen, Fujian 361005, China. E-mail addresses: rjxie@xmu.edu.cn (R-J Xie).

ABSTRACT

Heat treating is effective to enhance the thermal stability of the polymer derived SiC fibers through increasing the grain size and purifying the grain boundary. However, a long-term heat treatment usually causes serious damages to the fibers and finally sacrifices the tensile strength. In this work, we apply an ultrafast (5-30 s) and high temperature (1900-2100°C) heat treatment on the near stoichiometric SiC fibers (namely C3) by Joule heating. As compared with the conventional heating techniques, the ultrafast Joule heating yields evident grain growth but less fiber damage. At above 2000°C, an instantaneous decomposition of the surface SiC grains leading to grain size reduction and a non-monotonically grain size distribution along the fiber diameter, which also contributes to decrease the surface roughness. The C3 fibers heat treated at 2100°C for 15 s show excellent creep resistance when compared to some other commercial SiC fibers, and also keeps high tensile strength.

Keywords: Joule heating, SiC fiber, creep resistance, tensile strength, microstructure

1. Introduction

With the development of the aerospace industry, the hot section temperature of the

new generation aero engines is expected to reach 1400-1700°C, surpassing the survivability limit of nickel-based high temperature alloys (which can withstand up to 1100°C) [1, 2]. SiC fiber-reinforced SiC ceramic matrix composites (SiC_f/SiC CMCs), however, have advantages that satisfy the dual requirements of high strength and high-temperature resistance, which have the working temperature more than 200°C higher than the nickel-based alloys [3]. At the same time, the SiC_f/SiC CMCs are much lighter than metal alloys, higher oxidation resistance than carbon materials, and higher toughness, and reliability than ceramic materials. Furthermore, they have good corrosion resistance, wear resistance and microwave-absorbing abilities. Therefore, they have a variety of applications in fields of nuclear fusion, aerospace and high-temperature radar stealth technologies [4-6].

The general processing route from fibers to composites consists of several steps, such as the preparation of fiber preforms, introduction of interphases around fibers, and the matrix formation (densification) [7]. The thermo-mechanical properties of composites are greatly determined by the fibers, it is thus of great significance to prepare SiC fibers with better mechanical and thermal properties. SiC fibers were first synthesized by Yijima at the laboratory in 1974, and industrialized by Nippon Carbon in Japan in 1980 [6, 8]. Since then, some commercial SiC fibers have been developed, with the trademarks of Nippon, Tyranno, Sylramic, and etc. These products can be divided into three generations based on the composition and microstructure of fibers. Among them, the third generation SiC fibers are near chemistry stoichiometric, which therefore have better mechanical properties and higher thermal stability [9, 10].

Although the SiC fibers can retain good strength at high temperatures, they experience severe creep that will lead to the failure of fibers and even composites. The creep becomes more noticeable at temperatures higher than about 45% of the absolute melting point of ceramics [11]. Creep under high temperature and low load is primarily induced by the diffusion of atoms through grain boundaries and within the crystal lattice. This type of creep exhibits a high sensitivity to the grain size and the purity of grain boundaries. [12]. Among the three generations of SiC fibers, third generation ones possess the best creep resistance at high temperatures due to their near chemistry

stoichiometric nature, larger grain size, and higher grain boundary purity [8, 11, 13]. For example, the grain size obtained by TEM analyses is the sequence of Tyranno SA (~ 200 nm) > Sylramic-iBN (> 100 nm) > Sylramic (~ 100 nm) > Hi-Nicalon Type SA (HNLS) (~ 20 nm) [14, 15], which largely depends on the sintering temperature. However, the creep resistance behaviors is the sequence of Sylramic-iBN > HNLS > Tyranno SA > Sylramic [16]. Although the Tyranno SA and Sylramic fibers have a bigger grain size than HNLS, their creep resistance is lower due to the low purity of their grain boundaries [8]. In short, the larger grain size and purer grain boundaries endow SiC fibers with higher creep resistance.

High-temperature heat treatment is an effective way to improve the creep resistance of SiC fibers, which can increase the grain size and purify the grain boundary. Sha *et al.* [17] investigated the influence of heat treatment temperature on the creep behavior of three kinds of commercialized SiC fibers (*i.e.*, Hi-Nicalon, HNLS, and Tyranno-SA) under an Ar atmosphere, and found that the creep resistance of all SiC fibers was improved by heat treatment, which is mainly related to the grain size of β -SiC and the composition at or adjacent to the grain boundary. However, the heat treatment also reduces the strength of SiC fibers. The strength reduction is ascribed to the grain growth, defect formation and residual thermal stress [18]. Dicarlo *et al.* [19] treated the Sylramic SiC fibers at 1800°C in N_2 to obtain the Sylramic-iBN fibers. The Sylramic-iBN fibers show better creep resistance and thermal stability than the original ones due to the grain coarsening and grain boundary purification. Moreover, the heat-treated fibers retain a relatively high strength on account of the surface protection by boron nitride (BN). The formation of BN is attributed to the migration of excess boron to the surface followed by its reaction with N_2 . Gao *et al.* [20] studied the thermal behavior of second-generation KD SiC fibers in N_2 and Ar, and found that the heat treatment caused much larger strength degradation in Ar. The strength degradation is attributed to the grain coarsening and porous surface of the fibers, and the decomposition of SiC_xO_y and $\text{SiC}_x\text{N}_y\text{O}_z$ phases occurs more easily in Ar.

The heating rate also plays an important role in affecting the thermal behavior of SiC fibers. Shimoo *et al.* reported that the pyrolysis of SiC fibers at a faster heating rate

(e.g., 600°C/h) is beneficial to improving their strength [21]. Kim *et al.* [22] investigated the effects of the pyrolysis temperature and heating rate on the mechanical properties of SiC fibers, and addressed that a faster heating rate (e.g., 40°C/min) resulted in higher tensile strength and greater elasticity at room temperature. In our previous work, we performed rapid heat treatment on the BN-coated near stoichiometric SiC fibers at 1800°C for 60 seconds in Ar, and found that the creep resistance of the treated SiC fibers was better than that of the untreated fibers and even higher than that of the commercialized HNLS SiC fibers. Furthermore, it keeps excellent strength compared to the as-prepared one after being treated at 1500°C for 1 hour. These good performances of the treated SiC fibers are ascribed to the moderate grain growth and smooth surface after fast heat treatments. However, the influence of even higher temperature fast heat treatment and different holding times on the microstructure, morphology and mechanical properties of near stoichiometric SiC fibers has not been discussed systematically. [23].

In this work, we apply an ultrafast high temperature heat treatment on SiC fibers and investigate their structural evolution and mechanical properties.

2. Experimental section

2.1. Materials

The near chemistry stoichiometric SiC fibers used in this study were the same as those used in our previous work, which were commercially available from LEADASIA Co. Ltd. (Quanzhou, Fujian, China) and abbreviately named as C3 [23]. Some basic properties of the C3 fibers can be found in our previous work. The fiber is supposed to possess an oxygen content of 0.8% and a C/Si ratio of 1.07. Its density is measured as 3 g/cm³. A carbon-rich layer with a thickness of 40 nanometers is formed on the fiber surface. The fiber exhibits a strength of 4.1 GPa and a Young's modulus of 336 GPa. The grain size of the C3 fiber by TEM is 14.5 nm. They were similar to those of commercialized Hi-Nicalon Type S (HNLS) produced by Nippon Carbon Inc. [24].

2.2. Heat treatment

A single C3 fiber was placed between two flexible sheets of carbon paper, and the end of the carbon paper was connected to two electrodes of the Joule heating equipment

(JSJ150-II, Hefei, China). The C3 fibers were heat treated at varying temperatures (*i.e.*, 1900, 2000 and 2100°C) for different holding times (*i.e.*, 5, 15 and 30 seconds) under the nitrogen (99.999% in purity) atmosphere. The temperature was measured by an infrared high-temperature thermometer (CK-7030A-MJ, Xi'an, China).

2.3. Characterizations

The field emission scanning electron microscopy (SEM, SU-70, Hitachi, Japan) and transmission electron microscopy (TEM, JEM-2100F, JEOL, Japan) were used in combination with energy dispersive spectroscopy (EDS) for microstructural observations and compositional determination of SiC fibers. Samples for TEM observations were prepared by a focusing ion beam system (FIB, NB5000, Hitachi, Japan). The phases of fibers were identified by an X-ray diffractometer (XRD, D8-A25, Bruker-Axs, USA).

In addition, the grain size of SiC in the fibers was observed and then statistically measured based on the high-resolution transmission electron microscopy (HRTM) images. Grain size measurements were performed manually using the ImageJ software (more than 40 particles were counted and then averaged).

2.4. Mechanical properties test

The high-temperature creep resistance of the fiber was determined by a modified bending stress relaxation (BSR) method that was used in our previous work [23, 25]. The modification was to fill the slit formed between the graphite clamp and graphite mandrel with carbon powders before placing the mandrel into the tube furnace to further minimize the oxidation degree of fibers under high temperatures. The oxidation may have a little impact on the measurement accuracy of creep resistance of the fibers. In this method, the creep resistance was evaluated by the stress relaxation ratio (m), which is defined as $m = 1 - R_0/R_a$, where R_0 is the radius of the graphite mandrel and R_a is the residual radius of the fiber after creep. The SiC fiber tow containing 10 single fibers were bent around a graphite mandrel with a fixed radius ($R_0 = 2$ mm) and held at constant strain. The mandrel was placed into a graphite clamp, and sprinkled very fine carbon dust between the mandrel and creep until the slit between them was filled, and then the graphite clamp was put into a tube furnace. Finally, they were heated at 1200,

1300, 1400 and 1500°C for 1 hour under 99.999% high purity argon gas, respectively. After cooling to the ambient temperature, the fibers were removed from the mandrel, and the residual radius R_a of the fiber loop was measured. The value of m was averaged over ten specimens in each test.

The tensile strength and elastic modulus of single fibers with a gauge length of 25 mm are examined by using an Instron-type test machine (Microtester-5948, England). The values of tensile strength and elastic modulus of each sample were averaged over at least 25 filaments.

3. Results and discussions

Fig. 1 shows the morphology and Energy dispersive spectroscopy (EDS) of the as-prepared SiC fiber (C3). C3 shows a smooth and dense surface containing small particles, and its fracture surface displays a typical brittle nature. The presence of

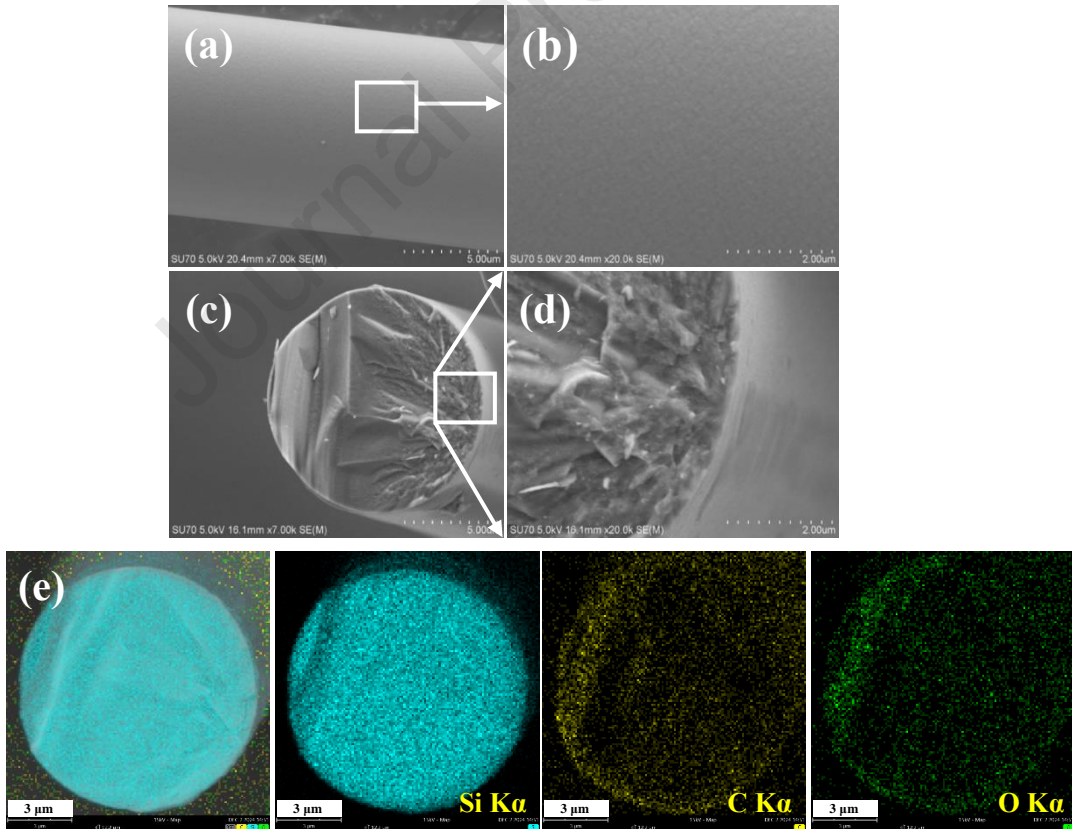
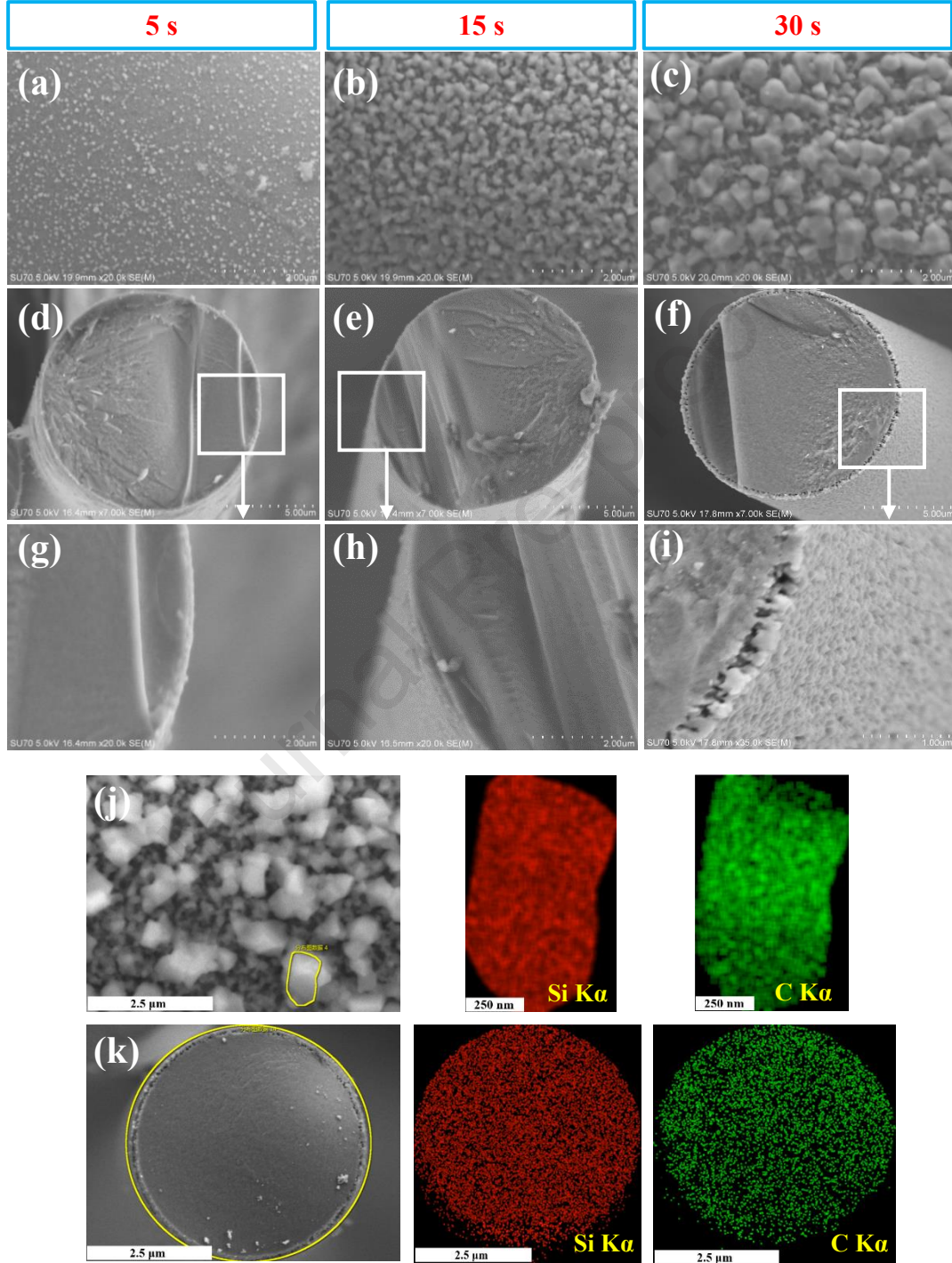


Fig. 1. Scanning electron microscopy (SEM) micrographs of the surface (a, b) and fracture morphology (c-d) of as-prepared C3 fiber. Energy dispersive spectroscopy (EDS) of C3 fiber (e).

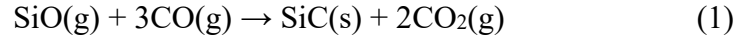
1 oxygen can be detected from the EDS in Fig. 1e.

2 After heat treatment at 1900°C, the island-like particles are produced on the
3 surface. These particles come together over time to form a discontinuous layer that



4 Fig. 2. Scanning electron microscopy (SEM) micrographs of the surface (a-c) and
5 fracture morphology (d-i) of C3 fiber treated at 1900 °C for different times. (a, d, g) 5s;
6 (b, e, h) 15s; (c, f, i) 30s; Energy dispersive spectroscopy (EDS) of C3 fiber treated at
7 1900°C for 30 s. (j) Surface scan; (k) Cross section scan.

looks like a fiber skin. Composition of these particles are mainly SiC, which can be verified by the EDS surface scanning images (Fig. 2j and 2k). These SiC particles grow more likely through the gas-phase reaction mechanism with the following equations [26, 27]:



At higher temperatures (*i.e.*, 2000 and 2100°C), pores instead of small particles are formed on the surface of the fiber. At the same time, from the cross-sectional

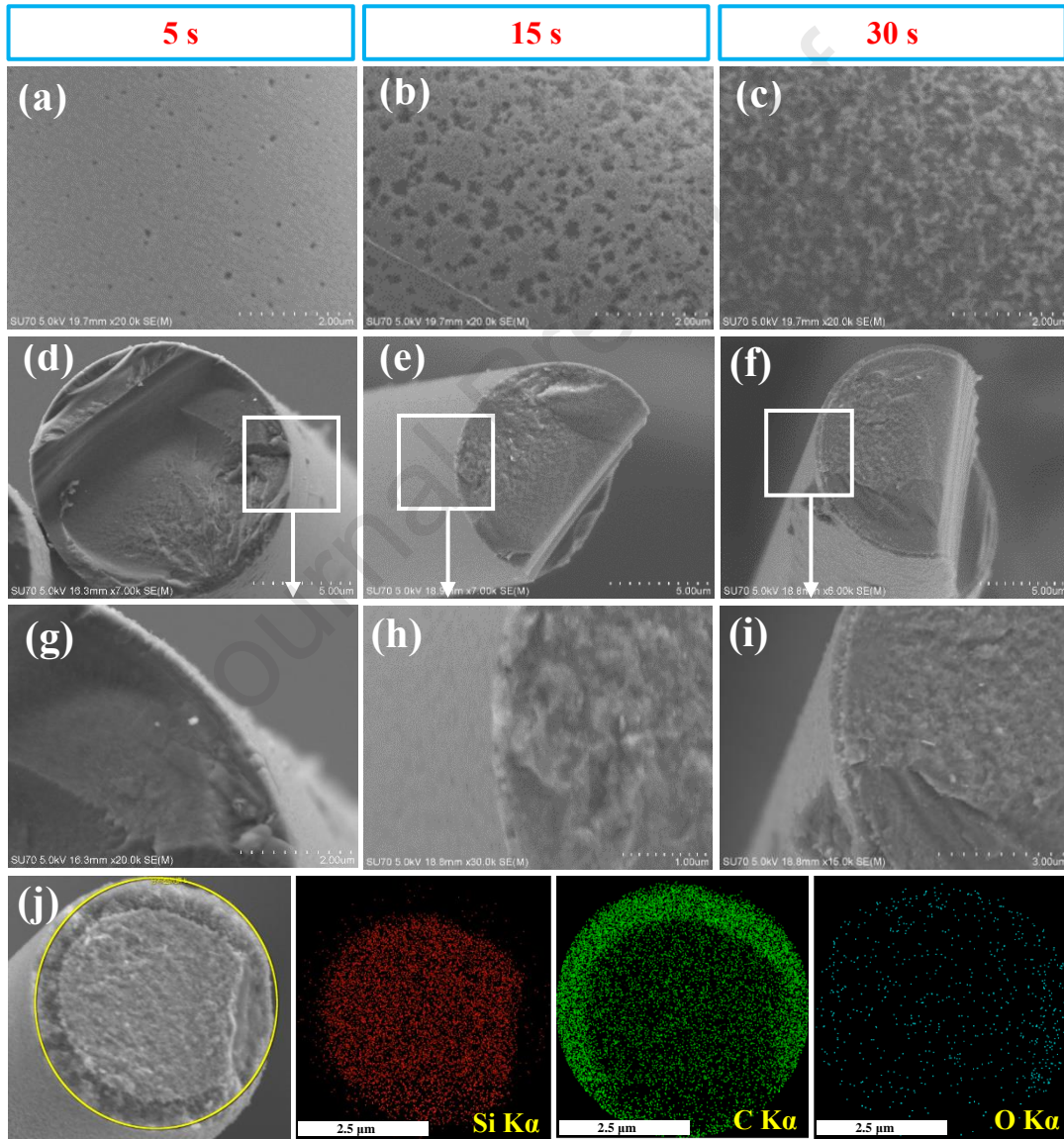
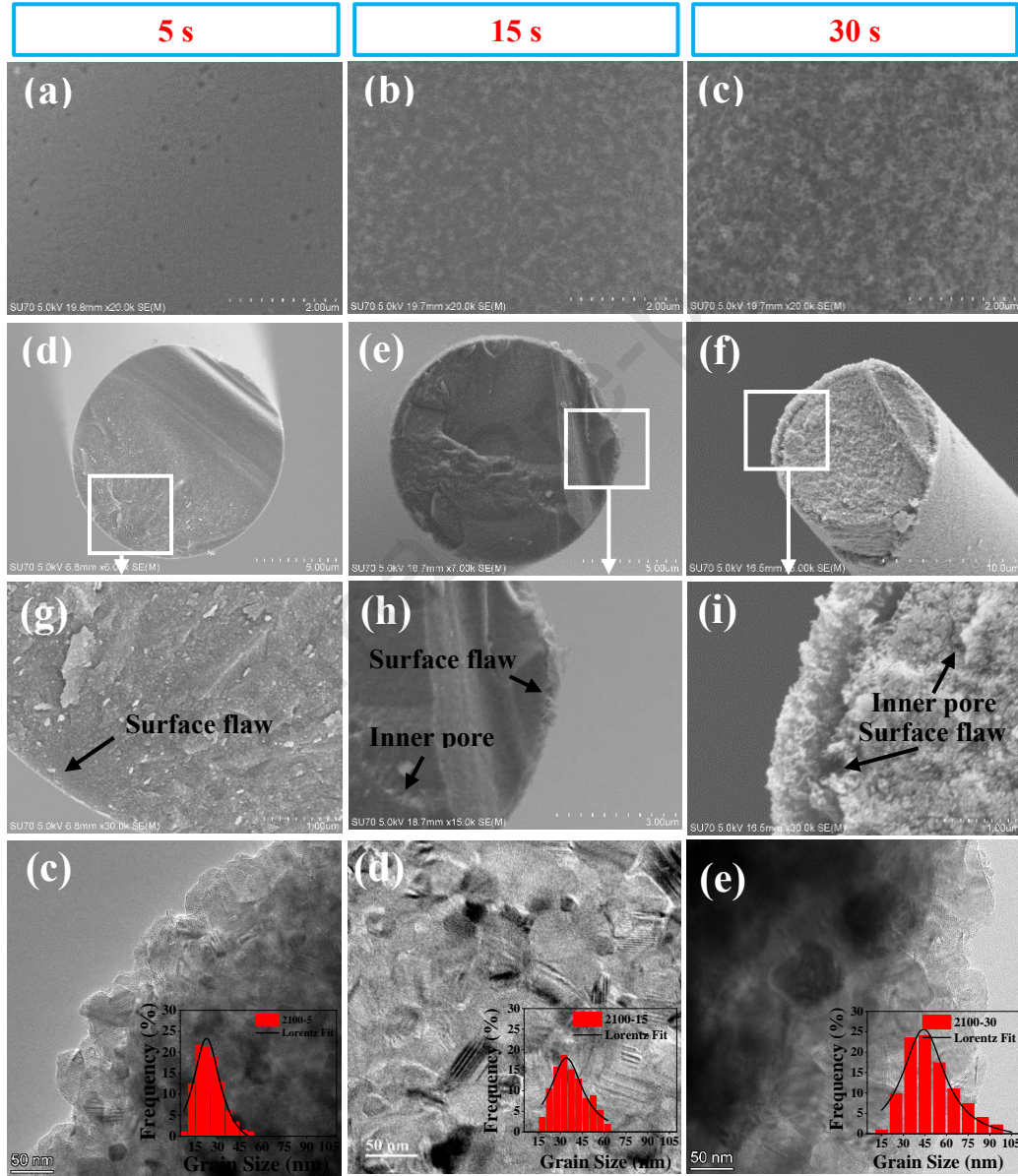


Fig. 3. Scanning electron microscopy (SEM) micrographs of the surface (a-c) and fracture morphologies (d-i) of the C3 fiber treated at 2000°C for different times: (a, d, g) 5 s; (b, e, h) 15 s; (c, f, i) 30 s; Energy dispersive spectroscopy (EDS) of the C3 fiber treated at 2000°C for 30 s (j).

1 image of the fiber, it can be clearly observed that the fiber surface is covered by a cortex,
 2 which we called the core/shell structure. The size and number of pores as well as the
 3 thickness of the shell on the fiber increase with time, as shown in Figs. 3 and 4. The
 4 composition of shell is mainly carbon and the core is mainly SiC, as given by the energy
 5 dispersive spectroscopy (EDS) in Fig. 3j. Meanwhile, the existence of a certain amount
 6 of uniformly distributed oxygen is observed from the EDS. However, the intensity of



7 Fig. 4. Scanning electron microscopy (SEM) micrographs of the surface (a-c) and
 8 fracture morphologies (d-i) of the C3 fibers treated at 2100°C for different times: (a, d,
 9 g) 5 s; (b, e, h) 15 s; (c, f, i) 30 s. (c, d, and e) Grain size distribution of the SiC fibers
 10 heat treated at 2100°C for different durations: (c) 5s; (d) 15s; (e) 30s.

the oxygen signal is relatively lower than that of the as-prepared sample (as shown in Fig. 1e), which indicates a decrease in oxygen content after high-temperature heat treatment. Carbon layer exhibits a porous structure, while the interior of SiC fiber is a relatively dense structure. Surface carbon layer is formed by the decomposition of surface SiC grains at ultra-high temperatures, as given by the following reaction [30, 31]:



Although, the ΔG of this reaction is >0 at those temperature ranges, however, this reaction is likely to proceed due to the effect of impurities (i.e., small amounts of oxygen, free carbon, and amorphous phase) in the SiC fibers, and more importantly the presence of high surface-active SiC nano-grains, which weaken the Si-C bond, causing SiC to decompose at low temperatures [30-32].

However, there are no significant changes in the fracture morphology of the fiber, except for the grain coarsening and the pore formation in the cross section when the fiber is treated at 2100°C for 30 s (Fig. 4f and Fig. 4i). The defects are produced between the SiC fiber and carbon skin are probably due to the difference in the thermal expansion coefficient of the SiC fiber and carbon ($4.5 \times 10^{-6}/^\circ\text{C}$ vs $2.0\text{-}3.0 \times 10^{-6}/^\circ\text{C}$) [26]. In addition, as can be seen from Fig. 4c-e, the grain size of the SiC fibers heat-treated at 2100°C increased monotonically with the treatment durations. Specifically, the grain sizes are 24.26, 36.83, and 49.11 nm for the duration of 5s, 15s, and 30s, respectively.

The high-temperature creep resistance of the C3 fibers, conducted at 1300°C for 1h, was verified by using the bend stress relaxation (BSR) method and evaluated by the stress relaxation parameter (m), as shown in Fig. 5a and Table 1. In this method, the creep resistance of the fibers increases with the m value increasing from 0 to 1. The m value of ~ 1 indicates the best creep resistance performance, whereas that of ~ 0 means the worse creep resistance of the fiber.

After heat treatment at high temperatures, all annealed samples show higher m values. In addition, the m value increases with the annealing temperature. On the other hand, with increasing the heat treatment time, the m value monotonically increases for the sample annealed at 1900°C , while it firstly increases and then remains almost

unchanged for the samples treated at 2000°C and 2100°C.

Specially for the SiC fiber heat-treated at 2100°C, the grain size increases with time, as depicted in Fig. 4.c-e, while the value of m remains essentially unchanged. For the SiC fiber heat-treated at 2100°C for 15 seconds, although its grain size is larger than that of the fiber heat-treated for 5 seconds, it maintains the same m value as the latter.

Table 1 Bend stress relaxation parameters (m) of the treated C3 fibers crept at 1300°C for 1h

Heat treatment temperature (°C)	Bend stress relaxation ratio m (Heat treatment period)			
	0s	5s	15s	30s
1900	0.6518	0.7196	0.7295	0.7940
2000	0.6518	0.8411	0.8385	0.8377
2100	0.6518	0.8635	0.8555	0.8655

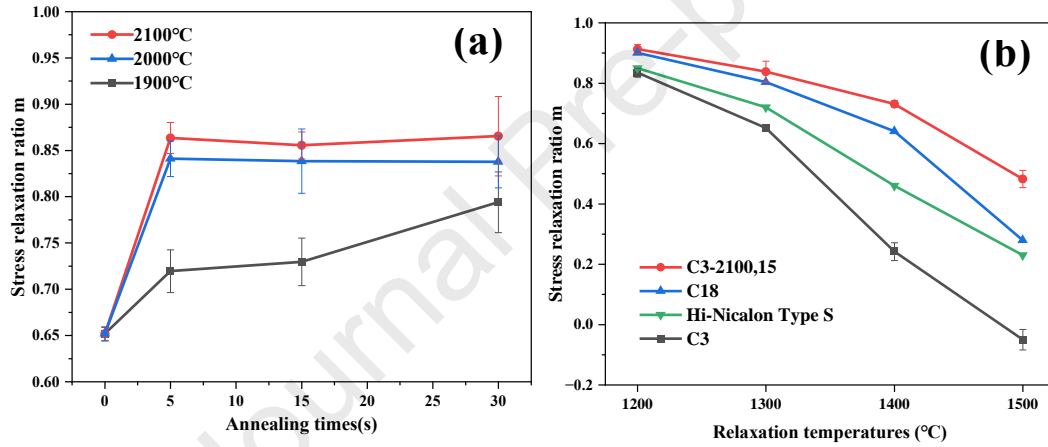


Fig. 5 (a) Bend stress relaxation parameters (m) of the heat treated C3 fibers crept at 1300°C for 1h. (b) Bend stress relaxation parameters (m) of four type fibers crept at different temperatures for 1 h.

This is most likely related to the formation of a carbon cortex on the fiber surface as shown in Figure 4h. The carbon cortex reduces the cross-section of the SiC fiber. Consequently, the SiC fiber bears a greater load per unit cross-sectional area during creep strain than the fiber with a thermal duration of 5 seconds. Moreover, the fiber with a duration of 30 seconds has an even larger grain size than those with durations of 5 and 15 seconds. However, it maintains the same m values as them. This is most probably due to its cavity structure as shown in Figs. 4f and 4I, which is favorable for grain boundary sliding. In short, it seems that the temperature of 2000°C is a threshold

one for activating a fast grain growth of the SiC fibers.

Figure 4(b) shows the bend stress relaxation parameters of four SiC fibers crept for 1h at different temperatures. The data of Hi-Nicalon Type S (HNLS) and C18 (C3 heat treated at 1800°C for 60 s) are derived from the literature [12]. The C3-2100,15 fiber, heat treated C3 at 2100°C for 15 s, has the maximal value among the tested fibers at all temperatures. High temperature creeping is mainly caused by the grain boundary migration that is sensitive to the grain size and grain boundary purification. The C3-2100,15 fiber exhibits larger grains and purer grain boundaries than the C18 and HNLS ones, showing the largest creep resistance among the four type fibers.

To investigate the influence of heat treatment time on the strength of SiC fibers, we measured the tensile strength of the fibers heat treated at 2100°C for varying times (Fig. 6a). One can see that the tensile strength of the fibers reduces monotonically with prolonging heat treatment time, and the strength retention of the fibers is 42.41, 37.73 and 15.47% for the heat treatment time of 5, 15 and 30 s, respectively. Increase the number and sizes of surface and inner defects with prolong the heat-treated times are responsible for the reduction in the tensile strength of the fibers. Although the strength of the C3 fiber decreases after the ultra-fast heat treatment, this result is still better than those reported in the literature [18], where the creep resistance of the HNLS SiC fiber is improved a little bit, but its strength is completely lost.

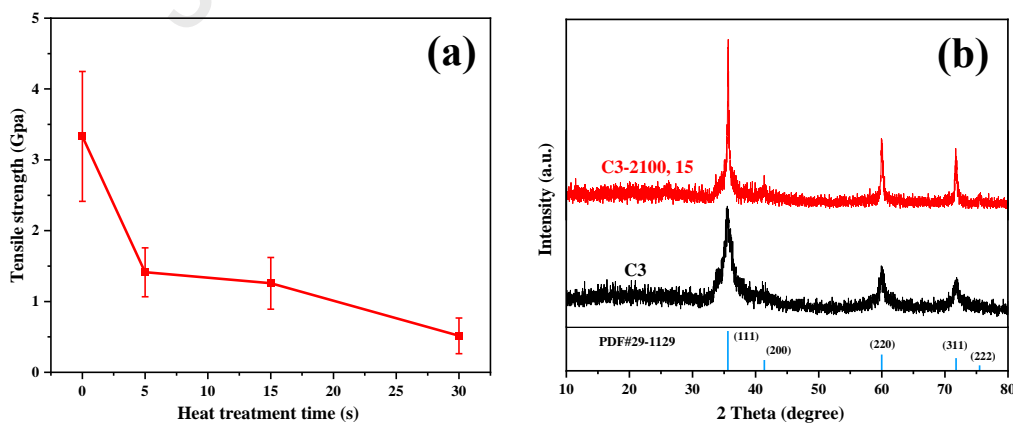
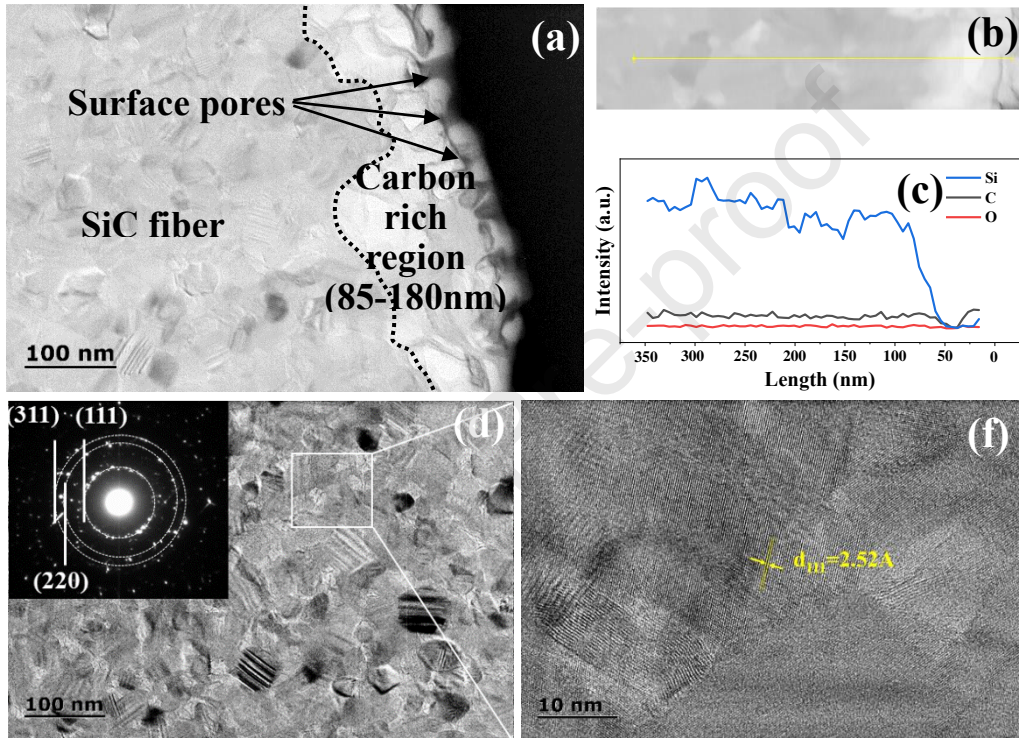


Fig. 6 (a) Tensile strength of the C3 fiber treated at 2100°C for different times. (b) XRD patterns of the C3 fiber and C3 fiber heat treated at 2100°C for 15 s (*i.e.*, C3-2100,15).

To gain a deep understanding why the rapid heat treatment at high temperature can improve the creep resistance of the fiber while keep relatively high tensile strength, the

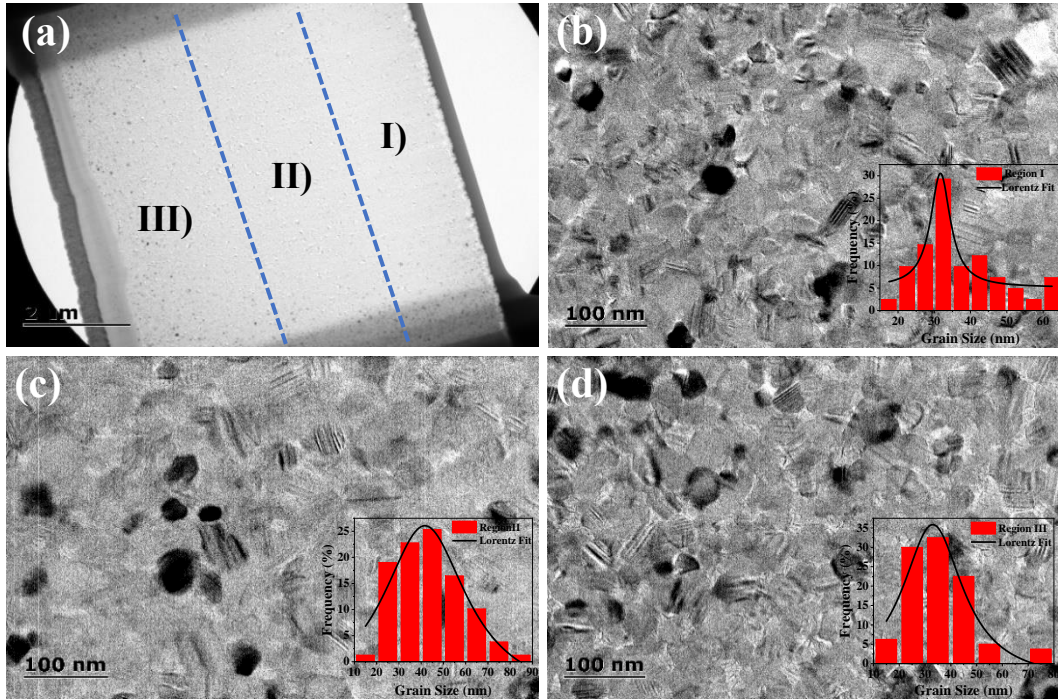
1 microstructure and composition of the C3 fiber and the fibers treated at 2100°C for 15
 2 s were investigated. As shown in Fig. 6b, the diffraction peaks at 35.6°, 41.2°, 60.2°,
 3 72.1° and 75.5° assigned to the (111), (200), (220), (311) and (222) crystal planes of β -
 4 SiC can be observed for both of the C3 and the heat-treated fibers, respectively.
 5 Compared with the C3 fiber, the diffraction peak strength of the heat-treated fiber is
 6 stronger, and the peak width is narrower, which implies an enhancement in crystallinity.



7 Fig. 7 (a) TEM image and (b, c) EDS plots of the C3 fiber treated at 2100°C for 15 s.
 8 Selected area electron diffraction (SEAD) (d) and high-resolution transmission electron
 9 microscope (HRTM) (f).

10 As given in Fig. 7a, some pores are formed on the surface of the fiber after heat
 11 treatment at 2100°C for 15s. These pores are caused by the decomposition and
 12 oxidations of SiC_xO_y and SiC phases on the surface of SiC fibers. The presence of these
 13 pores leads to the strength degradation. In addition, the carbon-rich region is formed by
 14 the decomposition of surface SiC grains and the evaporation of Si after high-
 15 temperature treatment, as discussed above. The diffraction rings are assigned to the
 16 (111), (220) and (311) crystal planes of β -SiC (Fig. 7c), which is consistent with XRD

1 results. The spacing between the two planes of (111) is 2.52 Å (Fig. 7d).



2 Fig. 8. TEM cross section images of the C3 fiber heat treated at 2100°C for 15 s (a) and
3 the grain size distribution in three regions: (b) region I, (c) region II and (d) region III.

4 The size of SiC grains was measured from the TEM micrographs (Fig. 8). A thin
5 sheet with a thickness of 20 nm and depth of 6.62 μm was sliced from the C3 fiber
6 heat treated at 2100°C for 15 s using FIB, and was then divided into three regions
7 from the surface to the core (*i.e.*, I, II and III), respectively. It is seen that the average
8 grain size of SiC in the fiber from surface to core is 37.08 nm (region I), 40.70 nm
9 (region II) and 35.68 nm (region III), respectively. The SiC grains in the middle
10 region have the largest size, which is different from that reported in the literature [23,
11 33], where the grain size of SiC near the fiber surface is the biggest after heat
12 treatment. Theoretically, the grain size near the surface should be larger than those
13 far away from the surface due to the temperature gradient. The unusual grain growth
14 observed in this study is most probably due to the decomposition of SiC grains near
15 the surface is much faster than the grain growth under the ultrafast heat treatment,
16 leading to smaller grains near the surface. Instead, the decomposition of SiC grains
17 in the middle region (region II) is less than that on the surface, therefor this region
18 exhibits larger grain size than the other two regions. The average grain size (37.82nm)

in the entire area of the fiber heat treated at 2100°C for 15s is approximately twice of the average grain size (*i.e.*, 14.5 nm) of the as-prepared C3 fiber [20].

Based on the above discussion, it can be concluded that the SiC fiber with near-chemistry stoichiometry after ultrafast heat treatment exhibits higher creep resistance, larger grain size, and greater crystallinity (which can be presumed to have higher grain boundary purity) compared to the as-prepared one. Additionally, it still maintains a relatively high tensile strength. The enhanced creep resistance of the heat-treated fiber can be ascribed to the enlarged grain size of SiC and improved purity at grain boundary. The relatively high strength of the SiC fiber after ultrahigh temperature heat treatment probably related to these factors: On the one hand, the shortening heat treatment period reduces the decomposition degree of the SiC_xO_y phases, which in turn reduces the surface and inner defects of the SiC fibers. In addition, the restriction of the SiC grain growth and formation of the carbon on the surface of SiC fiber helps to minimize and even to heal the surface defects. All of these results contribute to maintain the fiber strength. It can be predicted that the ultrafast heat treatment process introduced in this study is applicable to other types of SiC fibers, such as Tyranno and Sylramic fibers to improve the creep resistance while maintaining a high strength.

4. Conclusions

The ultrafast high-temperature heat treatment was conducted on the near-stoichiometric SiC fibers (*i.e.*, C3), and their microstructure and mechanical properties were investigated. The main results are summarized as follows:

- (1) The size of SiC grains and voids in the fiber increases with elevated temperatures and prolonged treating time, resulting in a decrease in tensile strength. The ultrafast heat treatment at 2100°C for 15s activates an instantaneous decomposition of SiC grains in the near surface, leading to a non-monotonically grain size distribution along the fiber diameter.
- (2) According to the BSR test results, all annealed fibers show higher creep resistance than the as-received one due to the grain coarsening and grain boundary

purification. With increasing the treating time from 5 s to 30 s, the creep resistance monotonically enhanced for the sample annealed at 1900°C, while it firstly enhances and then remains almost unchanged for the samples treated at 2000°C and 2100°C.

(3) The C3 fiber heat treated at 2100°C for 15 s have a better creep resistance than HNLS SiC fiber. At the same time, it maintains a relatively high strength (37.73% of the initial strength of 3.33GPa) due to the suppression on formation of surface defects.

Acknowledgements

This study was supported by the Natural Science Foundation of Xiamen, China (grant number 3502Z202373011), the Fundamental Research Funds for the Central Universities (grant number 20720220066), the National Key Project of China (grant number 2022-JCJQ-ZD-067-11).

Declaration of competing interest

The authors declare that they have no known competing financial interests or personal relationships that could have appeared to influence the work reported in this paper.

References

- [1] D. Zhu, Aerospace Ceramic Materials: Thermal, Environmental Barrier Coatings and SiC/SiC Ceramic Matrix Composites for Turbine Engine Applications, Nat. Aeronaut. Space Admin., Washington, Rep. NASA/TM-2018-219884, 2018.
- [2] A. Gloria, R. Montanari, M. Richetta, A. Varone, Alloys for Aeronautic Applications: State of the Art and Perspectives, Metals 9(6) (2019) 662.
- [3] D.B. Marshall, B.N. Cox, Integral Textile Ceramic Structures, Annu. Rev. Mater. 38 (2008) 425-443.
- [4] X.W. Yin, L.F. Cheng, L.T. Zhang, N. Travitzky, P. Greil, Fibre-reinforced multifunctional SiC matrix composite materials, Int. Met. Rev. 62 (2016) 117-172.
- [5] J. Binner, M. Porter, B. Baker, J. Zou, V. Venkatachalam, V.R. Diaz, A. D'Angio, P. Ramanujam, T. Zhang, T.S.R.C. Murthy, Selection, processing, properties and applications of ultra-high temperature ceramic matrix composites, UHTCMCs – a review, Int. Mater. Rev. 65 (2019) 389-444.
- [6] H. Ohnabe, S. Masaki, M. Onozuka, et al., Potential Application of Ceramic Matrix Composites to Aero-Engine Components, Compos. Part A Appl. Sci. Manuf. 30 (1999) 489-496.
- [7] X. Zhang, X. Wang, W. Jiao, Y. Liu, J. Yu, B. Ding, Evolution from microfibers to nanofibers

- toward next-generation ceramic matrix composites: A review, *J. Eur. Ceram. Soc.* 43 (2023) 1255-1269.
- [8] A. R. Bunsell, A. Piant, A review of the development of three generations of small diameter silicon carbide fibres, *J. Mater. Sci.* 41 (2006) 823-839.
- [9] M. Dong, G. Chollon, C. Labrugere, et al., Characterization of Nearly Stoichiometric SiC Ceramic Fibres, *J. Mater. Sci.* 36 (2001) 2371-2381.
- [10] T. Ishikawa, *Advances in Inorganic Fibers*, Springer, Berlin, 2005, pp. 109-144.
- [11] J. Lamon, Review: creep of fibre-reinforced ceramic matrix composites, *Int. Mater. Rev.* 65 (2019) 28-62.
- [12] J.J. Sha, J.S. Park, T. Hinoki, A. Kohyama, Bend stress relaxation of advanced SiC-based fibers and its prediction to tensile creep, *Mech. Mater.* 39 (2007) 175-182.
- [13] D. Schawaller, B. Clauß, M.R. Buchmeiser, Ceramic Filament Fibers – A Review, *Macromol Mater Eng* 297 (2012) 502-522.
- [14] M. Takeda, J. Sakamoto, A. Saeki, H. Ichikawa, Mechanical and Structural Analysis of Silicon Carbide Fiber Hi-Nicalon Type S. In: *Proceedings of the 20th Annual Conference on Composites, Advanced Ceramics, Materials, and Structures-B, Ceramic Engineering and Science Proceedings*, 17, Wiley, 1996, pp. 35-42.
- [15] D. Gosset, C. Colin, A. Jankowiak, T. Vandenberghe, N. Lochet, R. Hay, X-ray Diffraction Study of the Effect of High-Temperature Heat Treatment on the Microstructural Stability of Third-Generation SiC Fibers, *J. Am. Ceram. Soc.* 96 (2013) 1622-1628.
- [16] H. M. Yun, J. A. DiCarlo, Comparison of the Tensile, Creep, and Rupture Strength Properties of Stoichiometric SiC Fibers, *Ceram. Eng. Sci. Proc.* 20 (1999) 259-272.
- [17] J.J. Sha, J.S. Park, T. Hinoki, A. Kohyama, Heat treatment effects on creep behavior of polycrystalline SiC fibers, *Mater Charact* 57 (2006) 6-11.
- [18] J.J. Sha, T. Nozawa, J.S. Park, Y. Katoh, A. Kohyama, Effect of heat treatment on the tensile strength and creep resistance of advanced SiC fibers, *J. Nucl. Mater.* 329-333 (2004) 592-596.
- [19] J. A. DiCarlo, Y. Hee, Methods for producing silicon carbide architectural preforms, US Patent. 201076871016B1, 2010.
- [20] S. Cao, J. Wang, H. Wang, High-temperature behavior and degradation mechanism of SiC fibers annealed in Ar and N₂ atmospheres, *J. Mater. Sci.* 51 (2016) 4650-4659.
- [21] T. Shimoo, K. Okamura, M. Ito, et al., High-Temperature Stability of Low Oxygen Silicon Carbide Fiber Heat-Treated Under Different Atmosphere, *J. Mater. Sci.* 35 (2000) 3733-3739.
- [22] T. E. Kim, K. E. Khishigbayar, K. Y. Cho, Effect of heating rate on the properties of silicon carbide fiber with chemical-vapor-cured polycarbosilane fiber, *J. Adv. Ceram.* 6 (2017) 59-66.
- [23] S. Zhang, Z. Zhong, Y. Hua, S. W. Li, et al., Properties of super heat-resistant silicon carbide fibres with in situ BN coating, *J. Eur. Ceram. Soc.* 42 (2022) 6404-641.
- [24] M. Takeda, J. Sakamoto, Y. Imai, H. Ichikawa, T. Ishikawa, Properties of stoichiometric silicon carbide fiber derived from polycarbosilane. In: *Proceedings of the 18th annual conference on composites and advanced ceramic materials-A, Ceramic Engineering and Science Proceedings*, 15, Wiley, 1994, pp. 133-141.
- [25] G. N. Morscher, J. A. DiCarlo, A Simple Test for Thermomechanical Evaluation of Ceramic Fibers, *J. Am. Ceram. Soc.* 75 (1992) 136-140.
- [26] J.J. Sha, T. Hinoki, A. Kohyama, Microstructural characterization and fracture properties of SiC-based fibers annealed at elevated temperatures, *J. Mater. Sci.* 42 (2007) 5046-5056.

- [27] S. Cao, J. Wang, H. Wang, Formation mechanism of large SiC grains on SiC fiber surfaces during heat treatment, *CrystEngComm* 18 (2016) 3674-3682.
- [28] W.D. Kingery, H.K. Bowen, D.R. Uhlmann, *Introduction to Ceramics*, second ed., Wiley, New York, 1976.
- [29] Y.-s. Wang, X.-z. Wang, Y.-d. Wang, Effects of the Ar flow rate on the composition, structure, and properties of near-stoichiometric SiC fibres that were annealed at 1600°C, *Ceramics International* 48(17) (2022) 24571-24581.
- [30] Y. Gou, H. Wang, K. Jian, Formation of carbon-rich layer on the surface of SiC fiber by sintering under vacuum for superior mechanical and thermal properties, *J. Eur. Ceram. Soc.* 37 (2017) 907-914.
- [31] Y. Zhang, J. Chen, D. Yan, S. Wang, G. Li, Y. Gou, Conversion of silicon carbide fibers to continuous graphene fibers by vacuum annealing, *Carbon* 182 (2021) 435-444.
- [32] Y. Zhang, T. Chen, J. Chen, Q. Zhang, Y. Gou, The effects of annealing atmosphere and intrinsic component on high temperature evolution behaviors of SiC fibers, *Materials Science and Engineering: A* 848 (2022) 143363.
- [33] Y. Zhang, C. Wu, Y. Wang, J. Chen, Y. Qiu, X. Yang, Y. Gou, A detailed study of the microstructure and thermal stability of typical SiC fibers, *Mater. Charact.* 146 (2018) 91-100.

Table 1 Bend stress relaxation parameters (m) of the treated C3 fibers crept at 1300°C for 1h

Heat treatment temperature (°C)	Bend stress relaxation ratio m (Heat treatment period)			
	0s	5s	15s	30s
1900	0.6518	0.7196	0.7295	0.7940
2000	0.6518	0.8411	0.8385	0.8377
2100	0.6518	0.8635	0.8555	0.8655

Declaration of Interest Statement:

The authors declare that they have no known competing financial interests or personal relationships that could have appeared to influence the work reported in this paper.